Multiple-Instabilities in Magnetized Plasmas with Density Gradient and Velocity Shears

Makoto SASAKI[1,2], Naohiro KASUYA[1,2], Shinichiro TODA[3], Takuma YAMADA[2,4], Yusuke KOSUGA[1,2], Hiroyuki ARAKAWA[5], Tatsuya KOBAYASHI[3], Shigeru INAGAKI[1,2], Akihide FUJISAWA[1,2], Yoshihiko NAGASHIMA[1,2], Kimitaka ITOH[2,3,6] and Sanae-I ITOH[1,2]

[1]*Research Institute for Applied Mechanics, Kyushu University, Kasuga 816-8580, Japan*
[2]*Research Center for Plasma Turbulence, Kyushu University, Kasuga 816-8580, Japan*
[3]*National Institute for Fusion Science, Toki 509-5292, Japan*
[4]*Faculty of Arts and Science, Kyushu University, Fukuoka 819-0395, Japan*
[5]*Teikyo University, Fukuoka 836-8505, Japan*
[6]*Institute of Science and Technology Research, Chubu University, Kasugai 487-8501, Japan*

(Received 24 May 2017 / Accepted 28 August 2017)

Multiple free energy sources for instabilities coexist in magnetized plasmas with density gradient and velocity shear. Linear stabilities are investigated, and the mutual relation between resistive drift wave, D'Angelo mode and flute mode is systematically clarified. By evaluating the linear growth rates, dominant instability is categorized in a parameter space. The parallel wavenumber spectrum could be used as a guideline for the identification of the instabilities.

Keywords: stability, flow shear, turbulence, transport, drift wave, D'Angelo mode, flute mode

DOI: 10.1585/pfr.12.1401042

1. Introduction

Multiple free energy sources for instabilities coexist in magnetized plasmas with density gradient and velocity shear. Density and temperature gradients destabilize drift wave type instabilities such as resistive drift wave, and ion temperature gradient mode [1]. Inhomogeneous flows such as poloidal mean sheared flow, zonal flow and toroidal rotations are driven intrinsically [2–5] and/or externally [6–8]. Strong inhomogeneity of the perpendicular flow can be a free energy source of the Kelvin-Helmholtz (KH) instability [9–12] and interchange mode [13, 14]. When the parallel flow shear becomes strong, the parallel compression for ion acoustic waves can become negative to drive KH-type instability. This instability is called the D'Angelo mode [15, 16], which has been observed in basic plasma experiments [17]. Turbulence simulation and theory suggest the importance of the D'Angelo mode at scrape off layers and spherical tokamaks [18, 19]. The coexistence of the D'Angelo mode and drift wave has been observed [17]. On one hand, the drift wave induces the particle transport that reduces the density gradient, and simultaneously drive the momentum transport to form the parallel flow [20]. On the other hand, the D'Angelo mode relaxes the parallel flow gradient by momentum transport, and steepens the density gradient via the particle pinch effect [16]. Thus, a direct cross-interference between the particle and momentum transport occurs in a system where instabilities due to the density gradient and the flow inhomogeneities coexist. Therefore, the experimental identification of the instabilities among such modes is becoming increasingly important. Although the characteristics of these instabilities have been thoroughly investigated individually, the mutual relations between such instabilities need to be clarified in a systematic study.

Hence, in this study, we investigate the linear stability of magnetized plasmas in the presence of a density gradient, perpendicular flow curvature and parallel flow shear. The relationships between the resistive drift waves, D'Angelo and flute modes are clarified. In addition, a guideline for identifying such instabilities is presented here. The following parts of the paper are organized as follows. The basic model is described in Sec. 2, and analytical formulas for each instability are presented in Sec. 3. In Sec. 4, the mutual relations between the instabilities are described, and a summary is presented in Sec. 5.

2. Model

We consider slab plasmas with a density gradient, perpendicular flow curvature and parallel flow shear in a simple geometry where the magnetic field is homogeneous. This situation corresponds to those of the basic plasma experiments [6, 7, 17]. The direction of the magnetic field is chosen to be z-direction, and the direction of the gradient of the density is set to be x-direction. A three-field reduced fluid model is used, which is based on the Hasegawa-

author's e-mail: sasaki@riam.kyushu-u.ac.jp

Wakatani model with coupling of the ion parallel flow [16], where the field $\boldsymbol{f} = (N, \phi, V)^T$ is calculated. Here, the density N, electrostatic potential ϕ, and the ion parallel velocity V are normalized by mean density, electron temperature and sound speed, respectively. We divide $\boldsymbol{f}$ into its mean and fluctuating components as $\boldsymbol{f} = \langle \boldsymbol{f} \rangle + \tilde{\boldsymbol{f}}$. We keep the terms due to spatial inhomogeneities of $\langle \boldsymbol{f} \rangle$ (which causes the instabilities). In this study, we focus on the linear properties of the instabilities with multiple free energy sources; hence, we investigate the linearized equation. The basic model equation, and the derivation of the linearized equation are given in Appendix.A. The linearized equation is as follows,

$$\partial_t \tilde{\boldsymbol{f}} + \mathcal{L}\tilde{\boldsymbol{f}} = 0. \tag{1}$$

The linear operator $\mathcal{L}$ is given as

$$\mathcal{L} = \mathcal{L}_1 + \mathcal{L}_2, \tag{2}$$

$$\mathcal{L}_1 = \begin{pmatrix} -D\nabla_\parallel^2 - \mu_N \nabla_\perp^2 & D\nabla_\parallel^2 & \nabla_\parallel \\ -D\nabla_\perp^{-2}\nabla_\parallel^2 & D\nabla_\perp^{-2}\nabla_\parallel^2 + \nu - \mu_\phi \nabla_\perp^2 & 0 \\ \nabla_\parallel & 0 & \nu - \mu_V \nabla_\perp^2 \end{pmatrix}, \tag{3}$$

$$\mathcal{L}_2 = \begin{pmatrix} \langle V \rangle \nabla_\parallel + \partial_x \langle \phi \rangle \partial_y & -\partial_x \langle N \rangle \partial_y & 0 \\ 0 & -\partial_x \langle \phi \rangle \partial_y + I & 0 \\ 0 & -\partial_x \langle V \rangle \partial_y & \langle V \rangle \nabla_\parallel + \partial_x \langle \phi \rangle \partial_y \end{pmatrix}, \tag{4}$$

where $\mathcal{L}_1$ is the operator that describes the geometry and physical properties of the plasma, and $\mathcal{L}_2$ is related to the spatial inhomogeneity of the density, the electrostatic potential, and the ion parallel flow. The density gradient, $\partial_x \langle N \rangle$, the parallel flow shear, $\partial_x \langle V \rangle$, and the curvature of the azimuthal flow, $\partial_x^3 \langle \phi \rangle$, drive the drift wave, the D'Angelo mode and the KH instability, respectively. The ion-neutral collision frequency is denoted by ν, $D = A/(\nu_{ei} + \nu_{en})$ is the parallel diffusivity of electrons, A is the ion-electron mass ratio, ν_{ei} is the electron-ion collision frequency, ν_{en} is the electron-neutral collision frequency, and μ_N, μ_ϕ, μ_V are the viscosities. Here, the time and space are normalized by the ion cyclotron frequency and the ion sound Larmor radius, respectively. The operator I, which is important for driving the flute mode, is given as

$$\begin{aligned} I = {} & \partial_x^3 \langle \phi \rangle \nabla_\perp^{-2} \partial_y + \partial_x \langle N \rangle \nabla_\perp^{-2} \partial_x \partial_t \\ & + \partial_x \langle N \rangle \partial_x \langle \phi \rangle \nabla_\perp^{-2} \partial_x \partial_y - \partial_x \langle N \rangle \partial_x^2 \langle \phi \rangle \nabla_\perp^{-2} \partial_y. \end{aligned} \tag{5}$$

Assuming the function form of the fluctuations as $\tilde{\boldsymbol{f}} = \sum_k \boldsymbol{f}_k \exp(-i\omega t + i\boldsymbol{k}\cdot\boldsymbol{x}) + c.c$, we obtain the eigen equation as

$$\sum_j \Delta_{ij} f_{k,j} = 0, \tag{6}$$

$$\Delta = -i\omega \boldsymbol{I} + \mathcal{L}_k. \tag{7}$$

Here, $\mathcal{L}_k$ is calculated from $\mathcal{L}$, where the derivatives, ∂_t and ∇ are replaced by $-i\omega$ and $i\boldsymbol{k}$. The dispersion relation is obtained as

$$\det \Delta = 0. \tag{8}$$

From the eigen equation, the eigenfunctions of the density and the parallel flow fluctuations are formally written as

$$\tilde{N}_k = \frac{\Delta_{32}\Delta_{13} - \Delta_{33}\Delta_{12}}{\Delta_{11}\Delta_{33} - \Delta_{13}\Delta_{31}} \tilde{\phi}_k, \tag{9}$$

$$\tilde{V}_k = \frac{\Delta_{31}\Delta_{12} - \Delta_{11}\Delta_{32}}{\Delta_{11}\Delta_{33} - \Delta_{13}\Delta_{31}} \tilde{\phi}_k. \tag{10}$$

The dispersion relation shown in Eq. (8) includes the free energy sources for the instabilities due to $\partial_x \langle N \rangle$, $\partial_x \langle V \rangle$ and $\partial_x^3 \langle \phi \rangle$.

3. Analytical Formulas for Instabilities

Based on the linear dispersion relation (8), we investigate the relationships between the multiple instabilities. In order to obtain analytical insights, we derive expressions for the eigenfrequencies of each instability in a limit of $\nu, \mu_N, \mu_\phi, \mu_V \to 0$, keeping the effects of the flow and the density gradient.

Equation (8) can be expressed in a limit of $\nu, \mu_N, \mu_\phi, \mu_V \to 0$.

$$\begin{aligned} & \left(Dk_\parallel^2\right)\left[\Omega\left\{\left(1 + k_\perp^{-2}\right)\Omega + k_\parallel \langle V \rangle - k_\perp^{-2}\omega_* - iI\right\}\right. \\ & \quad \left. + k_\parallel k_y k_\perp^{-2} \partial_x \langle V \rangle - k_\parallel^2 k_\perp^{-2}\right] \\ & \quad + i\left(k_\parallel^2 - \Omega^2\right)\left(\Omega + k_\parallel \langle V \rangle - iI\right) = 0, \end{aligned} \tag{11}$$

where $\Omega = \omega - k_y \partial_x \langle \phi \rangle - k_\parallel \langle V \rangle$ is the eigenfrequency with the Doppler shift by the perpendicular and parallel flows, and $\omega_* = -k_y \partial_x \langle N \rangle$ is the electron drift frequency.

Cases of $k_\parallel \neq 0$

Equation (11) can be rewritten as

$$\Omega^2 - \alpha\Omega - \beta - i\epsilon(\Omega) = 0, \tag{12}$$

$$\alpha = \frac{\omega_* - k_\perp^2 k_\parallel + i k_\perp^2 I}{1 + k_\perp^2}, \tag{13}$$

$$\beta = \frac{-k_\parallel k_y \partial_x \langle V \rangle + k_\parallel^2}{1 + k_\perp^2}, \tag{14}$$

$$\epsilon(\Omega) = \frac{k_\perp^2}{Dk_\parallel^2\left(1 + k_\perp^2\right)}\left(\Omega^2 - k_\parallel^2\right)\left(\Omega + k_\parallel \langle V \rangle - iI\right). \tag{15}$$

Assuming $Dk_\parallel^2 \gg \omega$ and neglecting the term I, we treat $\epsilon(\Omega)$ perturbatively. We expand the solution as $\Omega = \Omega^{(0)} + \Omega^{(1)} + \ldots$ with the ordering of $O(\Omega/Dk_\parallel^2)$. The lowest and first order solutions are obtained as

$$\Omega^{(0)} = \frac{1}{2}\left(\alpha \pm \sqrt{\alpha^2 + 4\beta}\right), \tag{16}$$

$$\Omega^{(1)} = i\frac{\epsilon(\Omega^{(0)})}{2\Omega^{(0)} - \alpha}. \tag{17}$$

i) $\beta \to 0$

When the parallel flow shear is small $\beta \to 0$, the unstable

solution can be expressed as

$$\omega \approx \frac{\omega_*}{1+k_\perp^2} - \frac{k_\perp^2 k_\parallel \langle V\rangle}{1+k_\perp^2} + k_y \partial_x \langle\phi\rangle + k_\parallel \langle V\rangle + i\frac{k_\perp^2 \omega_* (\omega_* + k_\parallel \langle V\rangle)}{D k_\parallel^2 \left(1+k_\perp^2\right)^2}, \quad (18)$$

which corresponds to the resistive drift wave (including the effects of the parallel and perpendicular flows). The real frequency is Doppler shifted by the velocity field as seen in the third and fourth terms of the right hand side of Eq. (18). The parallel mean flow induces an asymmetry in the growth rate with respect to the sign of $k_\parallel$. The growth rate of the mode satisfying $k_\parallel \langle V\rangle > 0$ becomes large, and that of the mode with $k_\parallel \langle V\rangle < 0$ becomes small.

ii) $|\beta| > \alpha/4, \beta < 0$

The D'Angelo mode becomes unstable when the parallel flow shear satisfies $\alpha^2 + 4\beta < 0$, which can be expressed in terms of the parallel velocity shear as

$$k_\parallel k_y \partial_x \langle V\rangle > k_\parallel^2 + \frac{\left(\omega_* - k_\perp^2 k_\parallel \langle V\rangle\right)^2}{4\left(1+k_\perp^2\right)}. \quad (19)$$

This condition corresponds to $\alpha^2 + 4\beta < 0$, where the unstable branch is obtained from $\Omega^{(0)}$. The eigenfrequency of the unstable branch is derived as

$$\omega \approx \frac{\omega_*}{2\left(1+k_\perp^2\right)} - \frac{k_\perp^2 k_\parallel \langle V\rangle}{2\left(1+k_\perp^2\right)} + k_y \partial_x \langle\phi\rangle + k_\parallel \langle V\rangle + \frac{2\epsilon(\Omega^{(0)})}{\sqrt{|\alpha^2+4\beta|}} + i\frac{1}{2}\sqrt{|\alpha^2+4\beta|}. \quad (20)$$

The effect of $\epsilon(\Omega^{(0)})$ contributes to the real frequency unlike the drift wave case. The necessary condition for the D'Angelo mode to become unstable is Eq. (19), where the $k_\parallel$-spectrum of the D'Angelo mode is completely asymmetry with respect to the sign of $k_\parallel$.

Case of $k_\parallel = 0$

The dispersion relation of the mode with $k_\parallel = 0$ is obtained as

$$\Omega = iI. \quad (21)$$

The eigenfrequency can be expressed as

$$\omega \approx k_y\left\{\partial_x\langle\phi\rangle + k_\perp^{-2}\left(\partial_x^3\langle\phi\rangle - \partial_x\langle N\rangle\partial_x^2\langle\phi\rangle\right)\right\} + i\left(-k_x k_y k_\perp^{-4}\partial_x\langle N\rangle\partial_x^3\langle\phi\rangle\right), \quad (22)$$

where $k_\perp^{-2}k_x\partial_x\langle N\rangle \ll 1$ is assumed. When $k_x k_y \partial_x\langle N\rangle\partial_x^3\langle\phi\rangle < 0$ is satisfied, the mode with $k_\parallel = 0$ becomes linearly unstable due to the coupling of $\partial_x\langle N\rangle$ and $\partial_x^3\langle\phi\rangle$. Note that this instability is different from the KH instability and the rotation driven interchange mode (RDI) [13]. In order to explain the relation of the instability obtained here with the conventional KH and RDI modes, the eigenequation Eq. (6) is rewitten as

$$k_\perp^2\tilde{\phi}_k + \partial_x\langle N\rangle i k_x\tilde{\phi}_k - \frac{k_y}{\omega - k_y\partial_x\langle\phi\rangle}\left(\partial_x^3\langle\phi\rangle + \partial_x\langle N\rangle\partial_x^2\langle\phi\rangle\right)\tilde{\phi}_k = 0. \quad (23)$$

Here, the KH and RDI modes are destabilized by the third and fourth terms, respectively. Note that the KH and RDI modes are stable when the radial eigenfunction is a plane wave, $e^{ik_x x}$. Radial eigenmode analysis is necessary to include these instabilities. In this study, we assume the the function form as $e^{ik_x x}$, and remove the KH and RDI. As seen from the dispersion relation Eq. (22), the instability we are considering is driven by the coupling between the density and vorticity gradients.

The eigenfunctions of the density and parallel velocity fluctuations are explained in Appendix. B; these are important for the experimental identification of the instabilities. The characteristics of the quasi-linear fluxes of the particle and parallel momentum are also discussed in this appendix.

4. Mutual Relations between the Instabilities in Parameter Space

We consider situations where several free energy sources for the instabilities coexist. The dispersion relation in Eq. (8) is a cubic equation, implying that it has three solutions. In order to understand the relationships between the drift wave, D'Angelo and flute modes, the dispersion relation is calculated as shown in Fig. 1. In the case of the pure drift wave, Fig. 1 (a), (c), which corresponds to the condition that the parallel flow shear and the gradient of the vorticity are not present, the purely symmetric solution in $k_\parallel$ is obtained. When the parallel flow shear exists, the symmetry in $k_\parallel$ is violated, and the unstable D'Angelo mode appears where the real frequency of the drift wave and the ion sound wave degenerate. The linearly unstable flute mode $k_\parallel = 0$ appears and the D'Angelo mode disappears when the vorticity gradient $\partial_x^3\langle\phi\rangle$ is present as shown in Fig. 1 (e), (f).

In order to obtain a guideline for identifying the instability, we present the characteristics of the mode spectra based on the linear growth rate. The parameters here are chosen to be similar to those of a basic plasma experiment on PANTA [17]. The plasma radius is $a = 10$ [cm], the device length in z-direction is $\lambda = 4$ [m], and $\langle V\rangle = 0.7, k_x = 1/a, \mu_N = \mu_V = 10^{-2}, \mu_\phi = 10^{-4}, \nu_{ei} = 500, \nu_{en} = 10, \nu = 3.5\times10^{-2}$. Treating $\partial_x\langle N\rangle$, $\partial_x\langle V\rangle$ and $\partial_x^3\langle\phi\rangle$ as parameters, the linear growth rate in the mode number space is shown in Fig. 2, which is expected to correspond to the mode spectra. We use the relation, $k_y = m/a/2$ and $k_\parallel = 2\pi n/\lambda$, where m and n are the perpendicular and parallel mode numbers, respectively. Figures 2 (a)-(c) are obtained by changing the density gradient with $\partial_x\langle V\rangle = -0.15$, and $\partial_x^3\langle\phi\rangle = 0$. Figure 2 (a) shows the

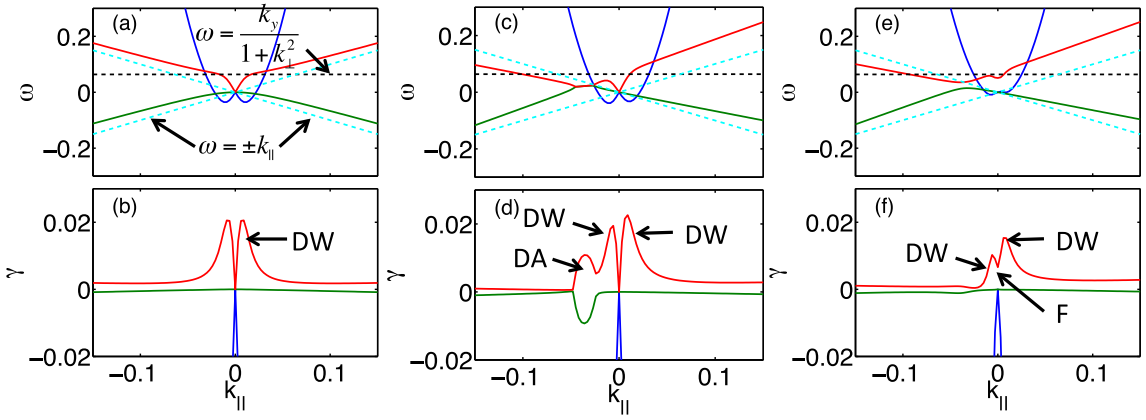

Fig. 1 Dispersion relations; (a), (b) pure drift wave, (c), (d) D'Angelo mode and drift wave, (e), (f) Flute and drift wave. Each case is calculated with $(\partial_x\langle N\rangle, \partial_x^3\langle\phi\rangle) = (0,0)$ for (a), (b), $(-0.2, 0)$ for (c), (d), and $(-0.2, 0.02)$ for (e), (f).

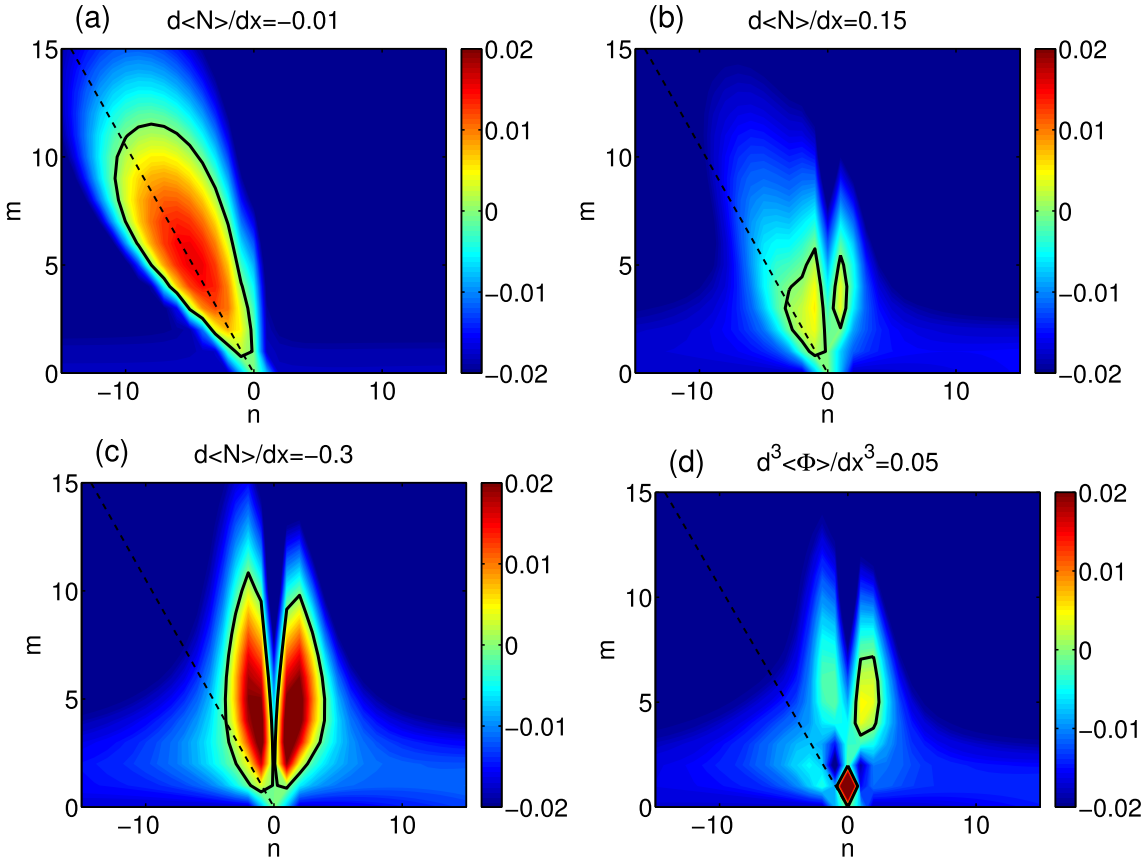

Fig. 2 Growth rate γ in (m,n)-space: (a) D'Angelo mode case, (b) intermediate mode of D'Angelo mode and drift wave, and (c) drift wave dominant case, and (d) flute mode dominant case.

characteristic spectrum of the D'Angelo mode, where the modes with $k_\parallel k_y \partial_x\langle V\rangle > 0$ are excited. This spectrum is asymmetry in n-space, where the n-spectrum width is wide ($\Delta n \sim 10$). Here, the regions where the linear growth rate is positive are indicated by the closed black lines. Note that the other area is filled with damped waves. The black broken line corresponds to the condition for the most unstable modes, $k_\parallel = k_y\partial_x\langle V\rangle/2$ [16]. When the density gradient becomes large, the D'Angelo mode becomes stable, and the resistive drift wave is destabilized as shown in Fig. 2 (c). The resistive drift wave is excited with finite small n, which is almost symmetric in the sign of n. The width of the n-spectrum is much narrower than that of the D'Angleo mode as $\Delta n \sim 1$. Weak asymmetry is observed in Fig. 2 (c), which is due to the parallel mean flow as described by Eq. (18). The intermediate case of the D'Angelo

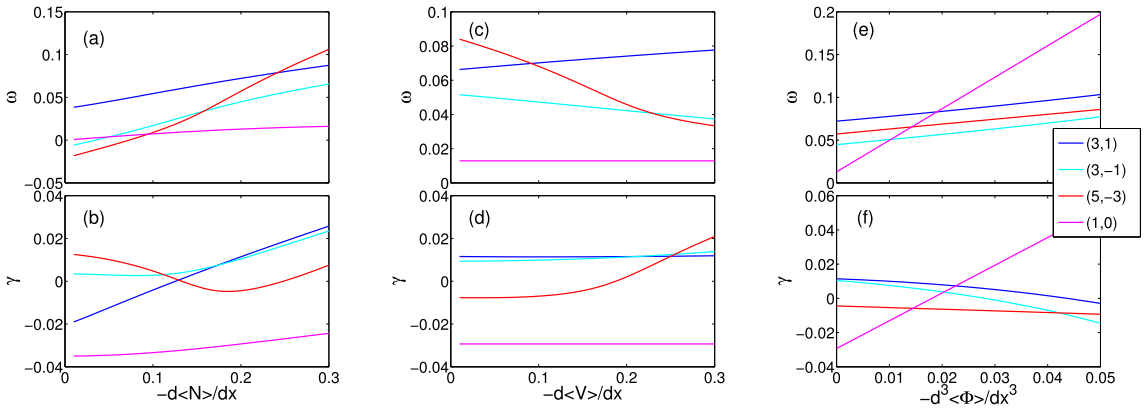

Fig. 3 Change of eigenfrequency and growth rate with the change of (a) (b) density gradient, (c) (d) parallel flow shear, and (e) (f) gradient of electrostatic potential curvature.

mode and the drift wave corresponds to Fig. 2 (b). The drift wave is observed at $n > 0$, and the intermediate mode appears at $n < 0$. Figure 2 (d) corresponds to the flute mode, which is obtained with $\partial_x^3\langle\phi\rangle = 0.05, \partial_x\langle V\rangle = 0$. The flute mode with $n = 0$ coexists with the drift wave with $n > 0$. In this case, the interference between the flute mode and the drift wave is expected.

Figure 3 illustrates the dependence of the real frequency and the growth rate of the instabilities on spatial inhomogeneities. The representative modes are selected as $(m, n) = (3, \pm 1), (5, -3), (1, 0)$ for the drift wave, D'Angelo and flute modes, respectively. The dependence on the density gradient is shown in Fig. 3 (a) and (b), which is calculated by using $\partial_x\langle V\rangle = -0.2, \partial_x^3\langle\phi\rangle = 0.05$. The frequency of the modes other than the flute mode increases with the density gradient. The growth rate of the drift wave constantly increases with $-\partial_x\langle N\rangle$. The growth rate of the D'Angelo mode decreases in the small density gradient cases, and increases to be drift wave-like mode in the high density gradient cases. Since the drift wave with the negative n satisfies the condition $k_y k_\parallel \partial_x\langle V\rangle > 0$, this mode is weakly driven by the parallel flow shear in addition to the density gradient. Thus, the mode with $n = -1$ becomes most unstable at the intermediate region of the D'Angelo mode dominant state and the drift wave dominant state. Figures 3 (c) and (d) show the dependence on the parallel flow shear. The real frequencies of the D'Angelo mode and the drift wave with the negative n become small with the parallel flow shear, and that of the drift wave with the positive n increases. The growth rates of the drift waves are not sensitive to the parallel flow shear. The dependence on the gradient of the potential curvature is shown in Figs. 3 (e) and (f). The frequency of the every instability increases with $\partial_x^3\langle\phi\rangle$. The growth rate of the drift waves becomes small with $\partial_x^3\langle\phi\rangle$, while that of the D'Angelo mode is not sensitive.

We focus on the behavior of the most unstable mode in the parameter space of $\partial_x\langle N\rangle, \partial_x\langle V\rangle$, and $\partial_x^3\langle\phi\rangle$. Figure 4 illustrates the parallel mode number of the most unstable

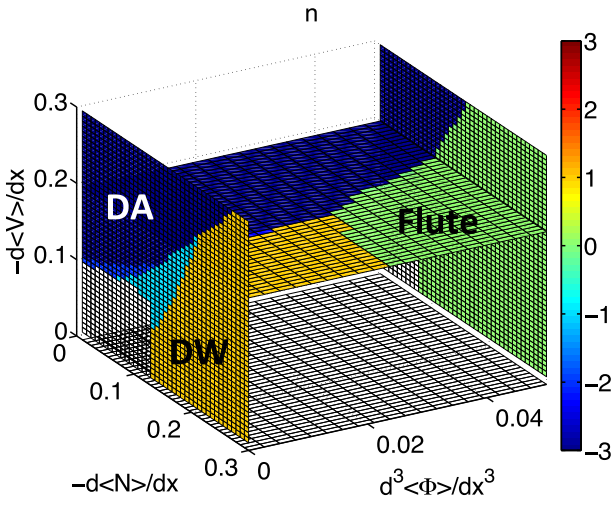

Fig. 4 Parallel mode number of the most unstable mode in parameter space. The drift wave and the D'Angelo mode are denoted by 'DW' and 'DA', respectively.

mode. In the region where the D'Angelo mode is dominant, the parallel mode number is $n < -2$, and is $n = 1$ in the drift wave dominant region. In its intermediate region, the drift wave with $n = -1$ can be most unstable. When the gradient of the potential curvature becomes large, the dominant mode changes from $n = 1$ to $n = 0$. The effect of the perpendicular flow on the D'Angelo mode is not so sensitive that the transition to the flute mode is not obtained in the weak density gradient cases. The real frequency and the growth rate of the most unstable mode are shown in Fig. 5. Although the boundary of the each dominant instability is not clear for the real frequency and growth rate as shown in Fig. 5, the boundary for the parallel mode number is clear. Thus, the parallel mode number is the key parameter for determining the type of the instability.

The characteristics of the spectra of each instability are summarized in Table 1, where it can be seen that the spectrum of the parallel mode number is important

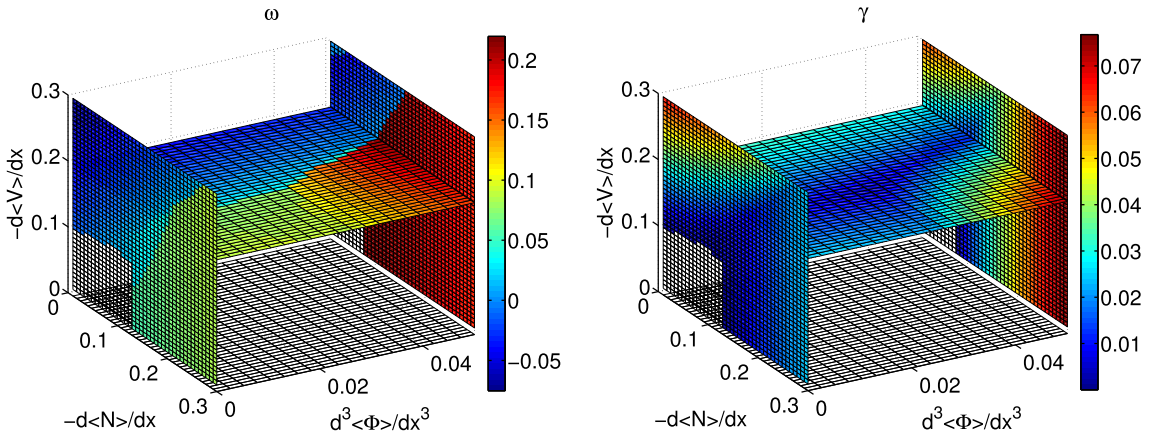

Fig. 5 (a) Real frequency and (b) growth rate of the most unstable mode in parameter space.

Table 1 Characteristics of each instability, where m and n are the azimuthal and axial mode numbers.

	necessary condition	n	Δn: spectrum width
drift wave	$n\langle V\rangle > 0$	$n = 1$ or -1	small
D'Angelo mode	$nm\langle V\rangle' > 0$	$\|n\|$: large	large
Flute mode	$\partial_x^3\langle\phi\rangle$: large	$n = 0$	small

for identifying the instabilities. Note that, in addition to the modes shown in the table, there is the intermediate mode in the region where the growth rates of the D'Angelo mode and the drift wave are similar. The sign of the parallel mode number of the intermediate mode is same as the D'Angelo mode, while the absolute mode number is $|n| = 1$, similar to the drift wave.

5. Summary

We systematically investigate the linear analyses of instabilities in the inhomogeneous magnetized plasmas with a density gradient, and parallel and perpendicular mean flows. The dispersion relation, which includes the multiple instabilities, is derived. The relationships between the resistive drift wave, D'Angelo and flute modes are clarified. Characteristics of the expected fluctuation spectra are discussed based on the linear growth rates. The dominant instability is categorized in a parameter space. The parallel mode number is the important parameter for identifying such instabilities.

Acknowledgments

This work was partly supported by a grant-in-aid for scientific research of JSPS, Japan (16K18335, 16H02442, 15H02155, 17H06089, 17K06994) and by the collaboration programs of NIFS (NIFS15KNST089, NIFS17KNST122) and of the RIAM of Kyushu University.

Appendix A. Derivation of Linear Dispersion Relation

The Hasegawa-Wakatani model with coupling of the ion parallel flow is considered. The basic model equation is given by

$$\partial_t \boldsymbol{f} + \mathcal{L}_1 \boldsymbol{f} = \mathcal{N}(\boldsymbol{f}, \boldsymbol{f}), \tag{A.1}$$

where the linear operator $\mathcal{L}_1$, and the nonlinear term $\mathcal{N}$ are given as

$$\mathcal{L}_1 = \begin{pmatrix} -D\nabla_\parallel^2 - \mu_N\nabla_\perp^2 & D\nabla_\parallel^2 & \nabla_\parallel \\ -D\nabla_\perp^{-2}\nabla_\parallel^2 & D\nabla_\perp^{-2}\nabla_\parallel^2 + \nu - \mu_\phi\nabla_\perp^2 & 0 \\ \nabla_\parallel & 0 & \nu - \mu_V\nabla_\perp^2 \end{pmatrix}, \tag{A.2}$$

$$\mathcal{N}(\boldsymbol{f}, \boldsymbol{f}) = \begin{pmatrix} [N, \phi] - V\nabla_\parallel N \\ \nabla_\perp^{-2}[\nabla_\perp^2\phi, \phi] - \nabla_\perp^{-2}\{\nabla N \cdot d_t\nabla_\perp\phi\} \\ [V, \phi] - V\nabla_\parallel V \end{pmatrix}, \tag{A.3}$$

where $[\phi, \ldots] = \partial_x\phi\partial_y - \partial_y\phi\partial_x$ is the convective derivative. We divide $\boldsymbol{f}$ into the mean and fluctuating components as $\boldsymbol{f} = \langle\boldsymbol{f}\rangle + \tilde{\boldsymbol{f}}$. Spatial inhomogeneity of $\boldsymbol{f}$ causes the instabilities; the density gradient, perpendicular flow curvature and the parallel flow shear destabilize the resistive drift waves, the flute modes and the D'Angelo modes, respectively. The nonlinear term is linearized as

$$\mathcal{N}(\boldsymbol{f}, \boldsymbol{f}) \approx -\mathcal{L}_2(\langle\boldsymbol{f}\rangle)\tilde{\boldsymbol{f}}. \tag{A.4}$$

The linearized equation is obtained as Eq. (1).

Appendix B. Eigenfunctions and Quasi-Linear Fluxes of Particles and Momentum

The quasi-linear fluxes of the particle and parallel momentum are evaluated by using the linear eigenfunction, Eqs. (9) and (10).

Case of $k_\parallel \neq 0$

Neglecting the viscosities $\mu_N = \mu_\phi = \mu_V = 0$, we derive the analytical expressions of the eigenfunctions with the assumption $Dk_\parallel^2 \gg \omega$ as

$$\tilde{N}_k \approx \Big\{1 + \frac{i}{Dk_\parallel^2\Omega}\Big(\Omega(\Omega-\omega_*) + k_\parallel k_y \partial_x\langle V\rangle - k_\parallel^2\Big)\Big\}\tilde{\phi}_k, \tag{B.1}$$

$$\tilde{V}_k \approx \Big[\frac{k_\parallel - k_y\partial_x\langle V\rangle}{\Omega} + i\frac{k_\parallel}{Dk_\parallel^2\Omega^2}\Big\{\Omega\,(\Omega-\omega_*) - k_\parallel^2 + k_\parallel k_y\partial_x\langle V\rangle\Big\}\Big]\tilde{\phi}_k. \tag{B.2}$$

The phase differences of the density and parallel flow fluctuations with the electrostatic potential are governed by Eqs. (B.1) and (B.2). The perpendicular flow affects the phase differences of the density and parallel flow through the Doppler shift. The parallel mean flow speed affects the phase relation through the Doppler shift, while the parallel flow shear directly affects the phase relations. The parallel flow fluctuation becomes large with the increase of the parallel flow shear as was observed in [21]. By using the above expressions, the quasi-linear fluxes are obtained as

$$\Gamma_x = \langle\tilde{N}\tilde{v}_x\rangle, \approx \sum_k \frac{k_y}{Dk_\parallel^2\Omega}\Big\{\Omega(\omega_*-\Omega) - k_\parallel k_y\partial_x\langle V\rangle + k_\parallel^2\Big\}|\tilde{\phi}_k|^2, \tag{B.3}$$

$$\Pi_{xz} = \langle\tilde{v}_x\tilde{V}\rangle, \approx \sum_k \frac{k_\parallel k_y}{Dk_\parallel^2\Omega^2}\Big\{\Omega(\omega_*-\Omega) - k_\parallel k_y\partial_x\langle V\rangle + k_\parallel^2\Big\}|\tilde{\phi}_k|^2, \tag{B.4}$$

where the radial velocity fluctuation is evaluated from the $E\times B$ drift as $\tilde{v}_x = -ik_y\tilde{\phi}$. The first term of the particle flux in Eq. (B.3) becomes positive when the drift wave is important, which leads to the outward particle flux. The second term contributes to the inward flux when the D'Angelo mode is important, $k_\parallel k_y\partial_x\langle V\rangle > 0$. The sign of the net particle flux is determined by the competition of these effects. Concerning to the parallel momentum flux, the first term, which is important for the drift wave case, can be positive and negative depending on the breaking of the symmetry in the sign of $k_\parallel k_y$. The second term, which is important for the D'Angelo mode case, is always negative, so that this term works as the relaxation of the flow profile. The detailed formulation of the net momentum flux is reported in [22].

Case of $k_\parallel = 0$

Similarly, the eigenfunction of the flute mode is obtained as

$$\tilde{N}_k \approx \frac{\omega_*}{\Omega}\tilde{\phi}_k, \tag{B.5}$$

$$\tilde{V}_k \approx -\frac{k_y\partial_x\langle V\rangle}{\Omega}\tilde{\phi}_k. \tag{B.6}$$

Then the fluctuation driven fluxes are derived as

$$\Gamma_x \approx -\sum_k \frac{k_y^2\gamma}{|\Omega|^2}|\tilde{\phi}_k|^2\partial_x\langle N\rangle, \tag{B.7}$$

$$\Pi_{xz} \approx -\sum_k \frac{k_y^2\gamma}{|\Omega|^2}|\tilde{\phi}_k|^2\partial_x\langle V\rangle, \tag{B.8}$$

where $\gamma = \mathrm{Im}\Omega$. Thus, in the case of the linearly unstable flute mode, the direction of the particle and parallel momentum fluxes are outward, and the density profile flattens. The transport coefficients of the particle and momentum fluxes take the same value in this case.

Depending on the type of instability, the effects of the fluctuation driven fluxes of the particles and momentum differ, and the properties of the background density and velocity field are sensitively affected. Since the fluctuation driven fluxes are determined from the summation of all excited modes, the competition and coexistence of the multiple instability become important to determine the background profiles. Nonlinear simulations are necessary for the study on the interaction between multiple instabilities [23].

[1] W. Horton, Rev. Mod. Phys. **71**, 735 (1999).
[2] P.H. Diamond *et al.*, Plasma Phys. Control. Fusion **47**, R35 (2005).
[3] A. Fujisawa *et al.*, Nucl. Fusion **49**, 013001 (2009).
[4] J.E. Rice *et al.*, Nucl. Fusion **47**, 1618 (2007).
[5] O.D. Gurcan *et al.*, Phys. Plasmas **14**, 042306 (2007).
[6] T. Yamada *et al.*, Nucl. Fusion **54**, 114010 (2014).
[7] T.A. Carter *et al.*, Phys. Plasmas **16**, 012304 (2009).
[8] D.M. Fisher *et al.*, Phys. Plasmas **24**, 022303 (2017).
[9] W. Horton *et al.*, Phys. Fluids **30**, 3485 (1987).
[10] W. Horton *et al.*, Phys. Plasmas **12**, 022303 (2005).
[11] H. Hasegawa *et al.*, Nature **430**, 755 (2004).
[12] E.J. Kim *et al.*, Phys. Plasmas **9**, 4530 (2002).
[13] P. Popovich *et al.*, Phys. Plasmas **17**, 102107 (2010).
[14] B.N. Rogers *et al.*, Phys. Rev. Lett. **104**, 225002 (2010).
[15] N. D'Angelo, Phys. Fluids **8**, 1748 (1965).
[16] Y. Kosuga *et al.*, Plasma Fusion Res. **10**, 3401024 (2015).
[17] S. Inagaki *et al.*, Sci. Rep. **6**, 22189 (2016).
[18] X. Garbet *et al.*, Phys. Plasmas **6**, 3955 (1999).
[19] W.X. Wang *et al.*, Nucl. Fusion **55**, 122001 (2015).
[20] P.H. Diamond, Nucl. Fusion **53**, 104019 (2013).
[21] N. Dupertuis *et al.*, Plasma Fusion Res. **12**, 1201008 (2017).
[22] Y. Kosuga, S.-I. Itoh and K. Itoh, Plasma Fusion Res. **11**, 1203018 (2016).
[23] M. Sasaki *et al.*, to be submitted to Phys. Plasmas.